nature neuroscience

# Synaptic mGluR activation drives plasticity of calcium-permeable AMPA receptors

Leah Kelly, Mark Farrant & Stuart G Cull-Candy

**In contrast with conventional NMDA receptor–dependent synaptic plasticity, the synaptic events controlling the plasticity of GluR2-lacking $Ca^{2+}$-permeable AMPA receptors (CP-AMPARs) remain unclear. At parallel fiber synapses onto cerebellar stellate cells, $Ca^{2+}$ influx through AMPARs triggers a switch in AMPAR subunit composition, resulting in loss of $Ca^{2+}$ permeabilty. Paradoxically, synaptically induced depolarization will suppress this $Ca^{2+}$ entry by promoting polyamine block of CP-AMPARs. We therefore examined other mechanisms that may control this receptor regulation under physiological conditions. We found that activation of both mGluRs and CP-AMPARs is necessary and sufficient to drive an AMPAR subunit switch and that by enhancing mGluR activity, $GABA_BR$ activation promotes this plasticity. Furthermore, we found that mGluRs and $GABA_BRs$ are tonically activated, thus setting the basal tone for EPSC amplitude and rectification. Regulation by both excitatory and inhibitory inputs provides an unexpected mechanism that determines the potential of these synapses to show dynamic changes in AMPAR $Ca^{2+}$ permeability.**





The rapid insertion or deletion of AMPARs is important for the expression of NMDA receptor (NMDAR)-dependent long-term synaptic plasticity[1,2], but only recently has attention focused on forms of plasticity that entail specific regulation of CP-AMPARs[3–8]. Such plasticity, involving GluR2-lacking CP-AMPARs, is of particular interest, as GluR2 is a key determinant of AMPAR function at central synapses[9]. Receptors that lack this subunit, in which glutamine (Q) has been switched to arginine (R) at the 'Q/R' editing site in the pore-lining region, are not only permeable to $Ca^{2+}$ ions, but also show a high single-channel conductance[10] and an inwardly rectifying current-voltage (*I-V*) relationship as a result of their voltage-dependent block by endogenous intracellular polyamines[11–14]. Accordingly, changes in the targeting of GluR2, both pre- and postsynaptically, shape the properties of excitatory postsynaptic currents (EPSCs)[3,15,16].

At cerebellar parallel fiber–stellate cell synapses, which express CP-AMPARs, but lack colocalized NMDARs[17], synaptic activity triggers a rapid incorporation of GluR2-containing $Ca^{2+}$-impermeable AMPARs (CI-AMPARs), generating a lasting reduction in postsynaptic $Ca^{2+}$ entry[3]. Although elevation of intracellular $Ca^{2+}$ following activation of CP-AMPARs is essential in this form of plasticity, the prolonged postsynaptic depolarization that accompanies parallel fiber activity under physiological conditions[18] will limit such postsynaptic $Ca^{2+}$-influx. This is a result of the enhanced CP-AMPAR channel block by polyamines[14] and reduced ionic driving force. Thus, the precise mechanisms underlying this form of plasticity remain unclear. We found that metabotropic receptors, which would allow an activity-dependent and voltage-independent increase in intracellular calcium, are important in this process.

In the cerebellum, parallel fiber activity excites stellate cells, which in turn provide feedforward inhibition onto neighboring stellate cells[19]. Parallel fiber stimulation thus results in activation of both ionotropic and metabotropic glutamate and GABA receptors in these cells[20–22]. Activation of $GABA_B$ receptors has been shown to enhance mGluR responses of Purkinje cells. Indeed, it has been proposed that interaction between these two types of metabotropic receptor may provide a mechanism for regulating parallel fiber synaptic plasticity[23]. The high level of spontaneous GABAergic input to stellate cells, arising from action potential firing in neighboring stellate cells[24,25], could facilitate a similar interaction.

We examined the factors governing rapid changes in AMPAR $Ca^{2+}$ permeability in cerebellar stellate cells and found that the activation of both mGluRs and $GABA_BRs$ drives the reduction in CP-AMPARs, which is triggered by a rise in intracellular $Ca^{2+}$. Furthermore, in the absence of external stimulation, block of either group 1 mGluRs or $GABA_BRs$ led to an increase in $Ca^{2+}$-permeable synaptic AMPARs, indicating that metabotropic receptors are normally tonically active and that both excitatory and inhibitory inputs therefore govern the dynamic change in subunit composition and $Ca^{2+}$ permeability of synaptic AMPARs at cerebellar stellate cell synapses.

## RESULTS

### mGluR activation causes a persistent change in EPSC rectification

To test whether mGluR activation participates in insertion of GluR2-containing AMPARs, we measured stellate cell EPSC properties following application of the group 1 mGluR agonist (*S*)-3,5-dihydroxyphenylglycine (DHPG, 50 μM) (**Fig. 1**). The *I-V* relationship of EPSCs became less rectifying in a few minutes (**Fig. 1a**,**b**); on average, in

Department of Neuroscience, Physiology and Pharmacology, University College London, London, UK. Correspondence should be addressed to S.G.C.-C. (s.cull-candy@ucl.ac.uk).

Received 18 November 2008; accepted 3 March 2009; published online 19 April 2009; doi:10.1038/nn.2309

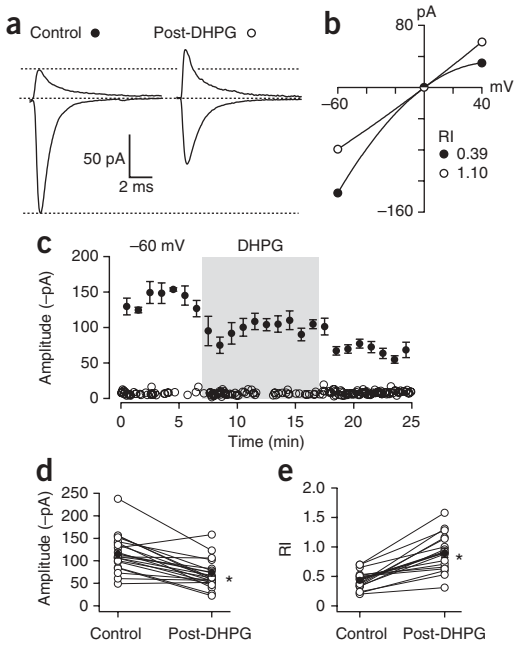


**Figure 1** The mGluR agonist DHPG induces a persistent synaptic depression and change in EPSC rectification. (**a**) Averaged parallel fiber–evoked EPSCs recorded at −60 and +40 mV before and after the application of 50 μM DHPG (10 min). Dashed lines indicate baseline and peak current for control EPSCs. (**b**) *I-V* relationships from data in **a**. Control EPSCs were inwardly rectifying (rectification index (RI) = 0.39 in this example); following DHPG application the *I-V* relationship became linear (rectification index = 1.1). (**c**) Time course of the effect of 50 μM DHPG on peak amplitudes of EPSCs at −60 mV in a single cell. Filled symbols represent means (averages of 1-min periods), and error bars represent s.e.m. Open symbols show response failures. Shaded area denotes the period of DHPG application. Control averages in **a** are from EPSCs recorded in the first 5 min illustrated (−60 mV) and in the preceding 5 min (+40 mV, data not shown). Likewise, post-DHPG averages in **a** are from EPSCs recorded in the last 5 min illustrated (−60 mV) and in the subsequent 5 min (+40 mV, data not shown). (**d**) Effect of DHPG on mean EPSC amplitude at −60 mV. (**e**) Effect of DHPG on rectification. In **d** and **e**, * denotes significant difference from control ($P < 0.0001$). In **d** and **e**, open symbols show individual cells, solid symbols show mean data and error bars represent s.e.m.

25 cells, the rectification index doubled, from 0.43 ± 0.04 to 0.82 ± 0.06 ($P < 0.0001$, Wilcoxon matched pairs test; **Fig. 1e** and **Supplementary Fig. 1** online). At negative potentials (–60 mV), where GluR2-lacking receptors contribute to the EPSC, DHPG produced a 37% reduction in EPSC amplitude (from –118 ± 7 pA in controls to –74 ± 7 pA after treatment, $n = 29$, $P < 0.0001$, Wilcoxon matched pairs; **Fig. 1d**). At +40 mV, EPSC amplitude remained unchanged or was slightly increased (**Fig. 1a**); on average EPSC amplitude was 31 ± 4 pA in control versus 33 ± 6 pA post-DHPG treatment ($n = 17$, $P = 0.766$, Wilcoxon matched pairs). These changes indicate that, following DHPG, EPSCs were mediated mainly by CI-AMPARs. Previous studies indicate that manipulations that alter rectification index are usually accompanied by a decrease in EPSC amplitude at negative potentials[3,5], possibly reflecting the lower single-channel conductance of CI-AMPARs compared with CP-AMPARs[10,14,26,27]. The effects of DHPG were readily blocked by the group 1 mGluR antagonists (+)-2-methyl-4-carboxyphenylglycine (LY367385, 100μM) and 2-methyl-6-(phenylethynyl)-pyridine (MPEP, 10μM) (see Methods) or by LY367385 alone (data not shown).

The effects of DHPG on EPSC properties were rapid and long lasting. Evoked EPSCs consistently decreased in amplitude following 10 min of treatment (**Fig. 1c**). This persisted after washout and for the duration of the recording (up to 1 h). In addition, EPSC failure rate was increased (**Fig. 1c**) from 0.18 ± 0.03 before DHPG to 0.35 ± 0.06 post-DHPG treatment ($n = 20$, $P = 0.013$). Typically, the change in failure rate would imply a presynaptic change, but it could reflect a selective postsynaptic action if some synapses express a high proportion of GluR2-lacking AMPARs that are rapidly removed[28].

### DHPG acts postsynaptically to change CP-AMPARs

To test whether the effects of DHPG were pre- or postsynaptic, we carried out several different experiments. First, we asked whether a change in rectification index could simply reflect a change in transmitter release, as might occur if varying the level of release resulted in activation of different populations of receptors. We compared rectification index values that were measured from spontaneous EPSCs (mostly unitary events) with evoked EPSCs in the same cells. In a set of untreated control cells, we found no significant difference in rectification index between spontaneous and evoked events (0.56 ± 0.03 and 0.53 ± 0.03, respectively; $P = 0.226$, $n = 29$ cells), suggesting that the measurement of rectification index was not influenced by the level of release. Second, we measured the paired-pulse ratio (PPR) of EPSCs before and after DHPG treatment (**Fig. 2a**). This provides a sensitive measure of any change in transmitter release probability. One possible confounding issue is that polyamine unblock of CP-AMPARs can give rise to postsynaptic facilitation with repetitive stimulation. However, our previous experiments suggested that this form of facilitation was unlikely to greatly affect PPR measurements from native AMPARs composed of homomeric GluR3 AMPARs (the main CP-AMPAR subtype present in stellate cells[14]) as a result of attenuation of polyamine block by transmembrane AMPAR regulatory proteins (TARPS). Although DHPG rapidly decreased EPSC amplitude, the PPR was not significantly altered (control, 2.30 ± 0.25; DHPG, 2.19 ± 0.19; $n = 12$, $P = 0.3013$, Wilcoxon matched pairs; **Fig. 2a**,**b**), indicating that the reduction in EPSC amplitude and rectification is unlikely to reflect decreased transmitter release. Third, we examined the effect of DHPG on miniature EPSCs (mEPSCs). mEPSC amplitude was rapidly and significantly decreased by 50 μM DHPG, consistent with a postsynaptic action (mEPSC amplitude at –60 mV reduced from –34 ± 2 pA to –27 ± 2 pA 10 min post-DHPG treatment, $n = 8$, $P = 0.005$). This probably represents an underestimate in the reduction, as the smallest events may be lost in the background noise.

To verify that the DHPG-induced change in EPSCs was postsynaptic and reflected a loss of CP-AMPARs, we examined the effect of the selective CP-AMPAR blocker philanthotoxin-433 (PhTx, (S)-*N*-[4-[[3-[(3-Aminopropyl)amino]propyl]amino]butyl]-4-hydroxy-α-[(1-oxobutyl)amino]benzenepropanamide tris(trifluoroacetate) salt, 5 μM). Externally applied philanthotoxin analogs are known to produce a voltage- and use-dependent block of CP-AMPAR channels at negative potentials. This block is slowly relieved when AMPARs are activated at depolarized potentials[29]. Because CP-AMPARs under these conditions may contribute to EPSCs at positive potentials, we restricted our analysis of the effects of PhTx to the measurement of EPSC amplitudes at negative potentials (**Fig. 2c**,**d**). Although PhTx significantly reduced the amplitude of control EPSCs (from –111.2 ± 7.1 to –68.4 ± 9.8 pA, $n = 6$, $P = 0.03$, Wilcoxon matched pairs), it had no significant effect post-DHPG in a separate set of cells (–74.7 ± 15.0 versus –89.4 ± 17.7 pA in PhTx, $n = 7$, $P = 0.36$; **Fig. 2c**). These results confirm that synaptic AMPARs are predominantly $Ca^{2+}$ impermeable following DHPG treatment, suggesting a rapid loss of CP-AMPARs from the postsynaptic membrane. Of note, the

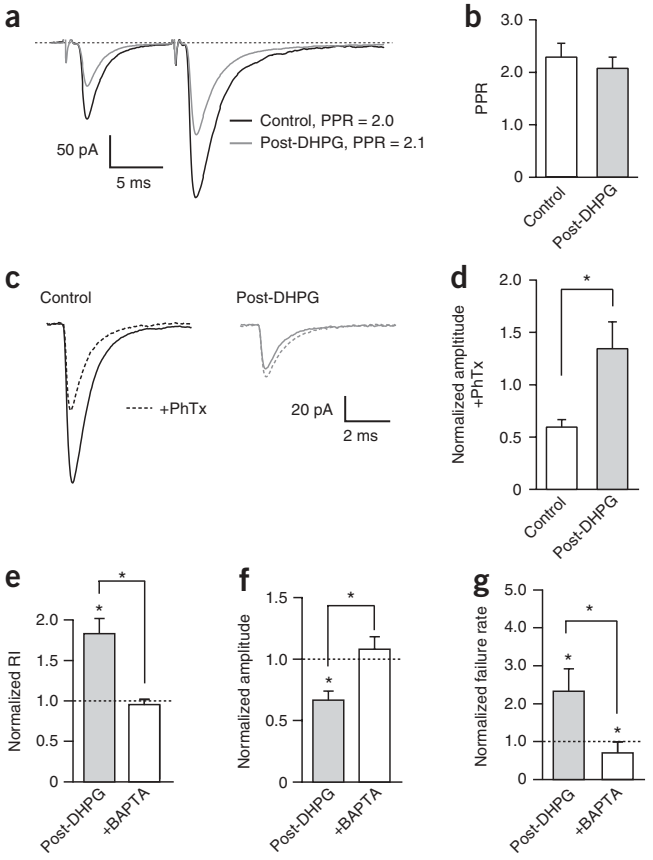


**Figure 2** DHPG action involves postsynaptic CP-AMPARs and $Ca^{2+}$ elevation. (**a**) Representative averaged parallel fiber–evoked EPSCs from a single cell showing paired-pulse facilitation (−60 mV, 10-ms interval) in control conditions and following application of 50 μM DHPG. Numbers denote PPR values for this cell. (**b**) Histogram of pooled PPR data from 12 cells. Error bars denote s.e.m. (**c**) Block of CP-AMPARs by PhTx was greatly reduced following DHPG. Representative mean EPSCs recorded before (solid lines) and after treatment with PhTx (5 μM, dashed lines) from a control cell (black) and a cell treated with DHPG (gray). (**d**) Histogram of pooled data from six control cells and seven cells post-DHPG. Asterisk denotes the significant difference in the action of PhTx in the two conditions ($P = 0.014$, Mann-Whitney U test). (**e**–**g**) Summary data comparing the effects of DHPG in different conditions. In the presence of BAPTA, DHPG no longer affected rectification index (0.60 ± 0.04 control versus 0.65 ± 0.04 post-DHPG, $n = 6$) or EPSC amplitude at -60 mV (–94 ± 9 versus –99 ± 6 pA, $n = 6$). Similarly, in the presence of BAPTA, failure rate was no longer increased by DHPG (failure rate was reduced from 0.32 ± 0.04 to 0.23 ± 0.03, $n = 8$, $P = 0.0288$). In each case, the effect of DHPG in recordings with BAPTA was significantly different from that produced by DHPG in control conditions (all $P < 0.05$). Error bars, here and throughout, denote s.e.m.

percentage reduction in EPSC amplitude at –60mV produced by PhTx (39%) was almost identical to that produced by DHPG (37%).

### Endocannabinoid synthesis and release is not required

Activation of group 1 mGluRs is known to lead to the elevation of intracellular $Ca^{2+}$, production of diacylglycerol (DAG) and release of endocannabinoids, which are widely involved in presynaptic plasticity in the CNS[30]. We sought to elucidate the mechanism of the DHPG-induced plasticity by testing the involvement of these well-characterized downstream processes. We first considered whether elevated intracellular $Ca^{2+}$ ($[Ca^{2+}]_i$) was required for the mGluR-mediated loss of GluR2-lacking AMPARs. EPSCs evoked at low frequency (0.5 Hz) with basal $Ca^{2+}$ buffering using EGTA (see Methods) showed no significant change in amplitude or rectification index over prolonged recordings ($P =$ 0.8125 and 0.875; see Methods). On the other hand, inclusion of 10 mM BAPTA in the pipette solution, to more rapidly buffer any rise in $[Ca^{2+}]_i$, produced a gradual and unexpected increase in EPSC rectification (after 30-min dialysis, rectification index had decreased from 0.59 ± 0.04 to 0.45 ± 0.05, $n = 9$, $P = 0.018$; **Supplementary Fig. 2** online). In the presence of BAPTA, DHPG was no longer able to elicit a decrease in EPSC rectification or amplitude (at negative potentials), and the increase in EPSC failure rate was abolished (**Fig. 2e–g**). This suggests that DHPG acts directly on mGluRs in stellate cells, mediating a rise in $[Ca^{2+}]_i$ that triggers a change in AMPAR subunit composition. The unexpected increase in EPSC rectification observed with BAPTA in the pipette solution was not seen in the presence of PhTx, suggesting that the BAPTA-induced change in rectification was a result of an increase in CP-AMPARs (**Supplementary Fig. 3** online). This raised the possibility that CP-AMPARs are normally downregulated, possibly by tonic mGluR activity (see below).

We next addressed whether the changes that we observed could be explained by the release of an endocannabinoid acting on CB1 receptors (CB1Rs) (**Fig. 3**). Inclusion of the CB1R blocker *N*-(piperidin-1-yl)-5-(4-iodophenyl)-1-(2,4-dichlorophenyl)-4-methyl-1 *H*-pyrazole-3-carboxamide (AM251) in the external solution throughout the experiment did not prevent the change in EPSC amplitude and rectification index that was seen after DHPG washout (**Fig. 3d,e**). We also examined inhibitors of DAG lipase, the enzyme that is required for the synthesis of the endocannabinoid 2-arachidonoylglycerol. Bath application of 100 μM 1,6-bis(cyclohexyloximino-carbonylamino) hexane (RHC-80267)[31] did not significantly alter the DHPG-induced changes in EPSC amplitude or rectification index (**Fig. 3d,e**). As the efficacy of RHC-80267 in blocking endocannabinoid release driven by $G_q$-coupled receptors has recently been questioned[32], we also examined the effect of tetrahyrolipstatin (THL), a highly selective DAG lipase inhibitor[32]. Inclusion of THL (2 μM) in the intracellular solution did not significantly modify the effect of DHPG (EPSC amplitude, $P$ = 0.448, Mann-Whitney U test; rectification index, $P$ = 0.86; **Fig. 3a–c**). Together with our data indicating that buffering of postsynaptic $Ca^{2+}$ with BAPTA inhibited the persistent change in EPSC amplitude and rectification index, these experiments support the view that this plasticity does not require the synthesis or release of cannabinoids, differentiating it from the CB1R-dependent form of plasticity that is expressed presynaptically at this synapse[31,33].

The plasticity that we observed appears to reflect changes in postsynaptic AMPARs. Previous studies suggest that such changes are suppressed by disrupting the interaction between GluR2 and the intracellular protein partner PICK-1 (refs. 5,34). However, it is not clear whether the loss of CP-AMPARs and delivery of new GluR2-containing receptors at stellate cell synapses depends on rapid translation processes. For example, it has recently been shown that mGluR1-mediated reversal of cocaine-induced changes in CP-AMPARs involves regulation of protein synthesis via an mTOR (phosphoinositide-3 kinase Akt mammalian target of rapamycin) pathway[27]. Consistent with a requirement for protein synthesis, we found that the DHPG-induced changes in EPSC amplitude and rectification index were blocked in slices bathed in 25 μM anisomycin (**Fig. 3f,g**).

### $GABA_BR$ activation promotes loss of CP-AMPARs

Stellate cells receive substantial GABA-mediated synaptic input from neighboring stellate cells[24,25]. As it has previously been found that activation of $GABA_BRs$ enhances parallel fiber–mediated mGluR

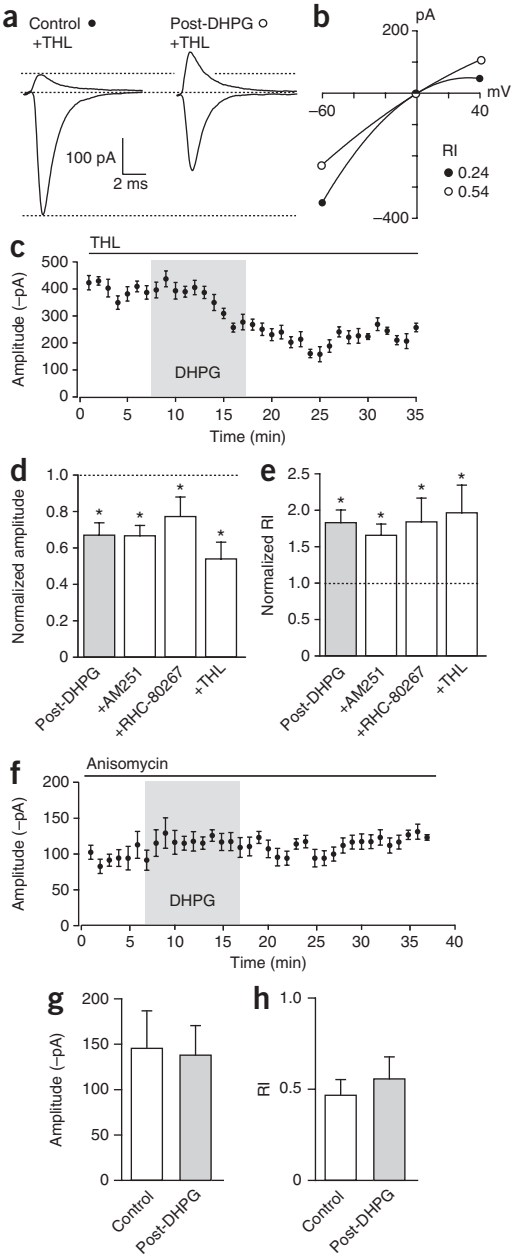


**Figure 3** DHPG-induced changes in rectification index do not involve cannabinoid release or CB1R activation, but require protein synthesis. (**a**) Inclusion of the DAG lipase inhibitor THL (3 μM) in the patch pipette did not block the effect of DHPG. Representative mean EPSC traces at +40 and −60 mV in control conditions and post-DHPG. (**b**) *I-V* relationship for data shown in **a**. The rectification indexes are shown for this cell. (**c**) Time course of the effect of DHPG on EPSC amplitude recorded at −60 mV (with THL, 3 μM). As for **Figure 1**, control averages in **a** are from EPSCs recorded in the first 5 min illustrated (−60 mV) and in the preceding 5 min (+40 mV, data not shown), whereas Post-DHPG averages are taken from the last 5 min illustrated (−60 mV) and the subsequent 5 min (+40 mV, data not shown). (**d**,**e**) Summary data comparing the effects of DHPG in different conditions. For comparison, normalized data for DHPG alone (from **Fig. 2e**,**f**) are shown in gray. The CB1R antagonist AM251 failed to block the effect of DHPG on EPSC amplitude (–100 ± 14 pA versus −63 ± 7 pA, $n = 9$, $P = 0.0088$, **d**) or rectification (0.33 ± 0.04 in control versus 0.53 ± 0.05 post-DHPG+AM251, $n = 8$, $P = 0.0022$, **e**). In both cases, the effect of DHPG in the presence of AM251 was not different from that of DHPG alone (all $P > 0.05$). Similarly, the DAG lipase inhibitors RHC-80267 and THL failed to block the effect of DHPG on EPSC amplitude and rectification index. EPSC amplitude was reduced from −215.5 ± 32.3 pA to –121.2 ± 32.7 pA ($P = 0.0156$, Wilcoxon matched pairs, $n = 7$) and rectification index was significantly increased from 0.42 ± 0.03 to 0.78 ± 0.14 ($P = 0.0313$, Wilcoxon matched pairs, $n = 6$) in the presence of RHC-80267 (30 μM). Mean EPSC amplitude decreased from –215.5 ± 32.3 pA to –121.2 ± 32.7 pA ($P = 0.0156$, Wilcoxon matched pairs $n = 7$) and rectification index increased from 0.41 ± 0.06 to 0.79 ± 0.15 ($P = 0.0210$, $n = 7$) in the presence of THL (2 μM). (**f**) Time course of the effect of DHPG on EPSC amplitude at –60 mV with anisomycin (25 μM) in bath. (**g**,**h**) Pooled data showing that anisomycin blocks the effect of DHPG on EPSC amplitude (–60 mV; –146.3 ± 40.6 versus –138.7 ± 31.83, $P = 0.5781$, Wilcoxon matched pairs, **g**) and rectification index (0.48 ± 0.08 versus 0.56 ± 0.11, $P = 0.1288$, $n = 7$, **h**). In **d**,**e**,**g** and **h**, error bars denote s.e.m. * indicates $P < 0.05$.

responses at cerebellar parallel fiber-Purkinje cell synapses[23], we considered whether activation of $GABA_B$ receptors in stellate cells might also influence the expression of CP-AMPARs. Application of the $GABA_B$ agonist baclofen (3 μM) resulted in a depression of transmitter release during and immediately following application, and also resulted in a decrease in EPSC amplitude and rectification that persisted after baclofen removal (**Fig. 4**). Baclofen produced a transient increase in EPSC failure rate, which was more pronounced than that seen with DHPG (**Fig. 4a**). Consistent with a reduction in transmitter release following activation of presynaptic $GABA_B$Rs, PPR was increased significantly in baclofen (from 1.91 ± 0.15 to 3.44 ± 0.41, $n = 6$, $P = 0.031$, Wilcoxon matched pairs) and returned to control values after washout (2.28 ± 0.13; **Fig. 4b**,**c**,**f**). Baclofen also caused a decrease in EPSC rectification, but this was not reversed on baclofen removal and appeared to be predominantly postsynaptic in origin (**Fig. 4d–f**). Supporting the idea that activation of postsynaptic $GABA_B$Rs promoted a loss of CP-AMPARs, we found that PhTx, when added after several minutes of baclofen treatment, no longer produced a significant reduction in EPSC amplitude (–51.5 ± 6.5 pA in baclofen, –41.4 ± 7.0 pA in PhTx, $n = 8$, $P = 0.1409$). Furthermore, inclusion of BAPTA in the patch pipette abolished the effect of baclofen on EPSC rectification (**Fig. 4g**). As expected, baclofen still produced a reversible reduction in EPSC amplitude in this condition as a result of activation of $GABA_B$Rs on parallel fiber terminals, although the reduction was slightly smaller than in the absence of BAPTA (**Fig. 4g**).

These data suggest that either $GABA_B$R activation elevates intracellular calcium *per se* or, more likely, that it augments an ongoing mGluR response. To determine whether cross-talk occurred between the metabotropic receptor types, as proposed for parallel fiber–Purkinje cell synapses[23], we examined the reciprocal affects of $GABA_B$R and mGluR antagonists on metabotropic receptor–mediated changes in AMPAR-mediated EPSCs. The DHPG-induced changes in EPSC amplitude, rectification index and failure rate were not significantly modified by the $GABA_B$R blocker CGP62349 (5 μM); EPSC amplitude was reduced (from –103.8 ± 12.7 to –70.9 ± 14.6 pA, $P = 0.0034$), rectification index was increased (from 0.34 ± 0.03 to 0.62 ± 0.08, $P = 0.0441$, Wilcoxon matched pairs) and the failure rate was increased (from 0.20 ± 0.05 to 0.48 ± 0.10, $P = 0.0019$). In contrast, we found that preincubation with LY367385 (100 μM) and MPEP (10 μM) significantly reduced the effect of baclofen on rectification (mean normalized change in rectification index with baclofen, 1.46 ± 0.10 versus 1.19 ± 0.06 in the presence of mGluR antagonists, $n = 15$, $P = 0.0244$). In these experiments, we first applied mGluR antagonists for ~20 min to allow the increase in EPSC amplitude (at –60 mV) and decrease in rectification index to reach a stable plateau before baclofen was added. This protocol was used to ensure that any effect of baclofen independent of mGluRs would not be masked. These results therefore

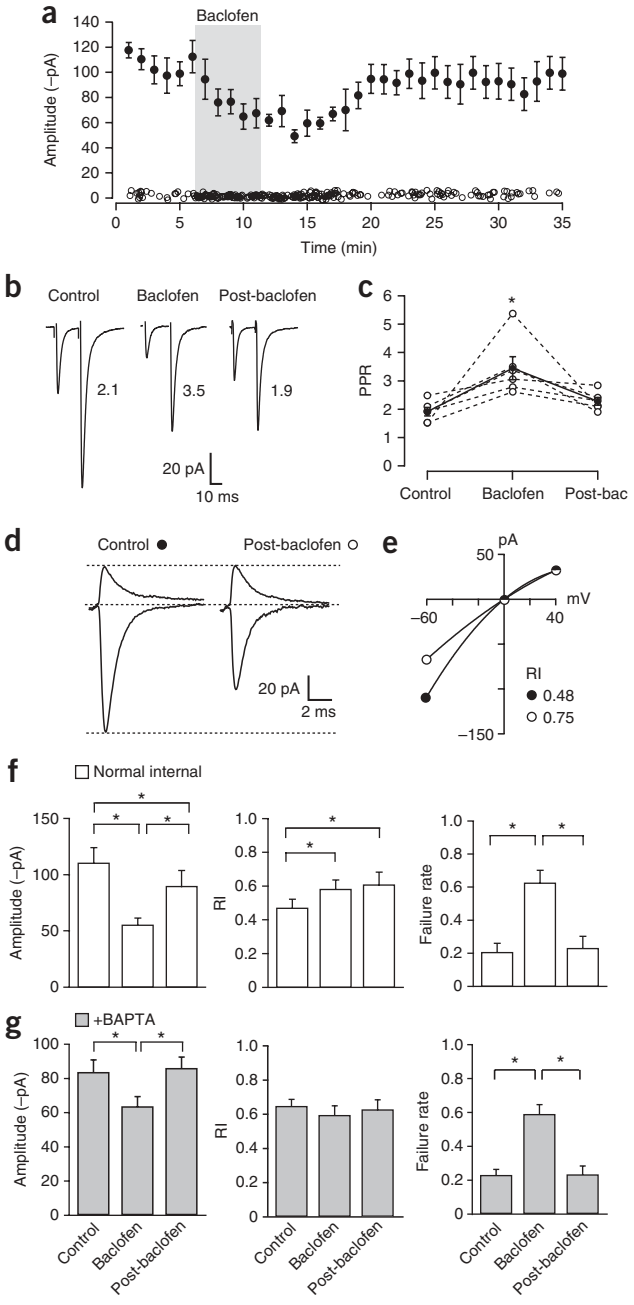


**Figure 4** Baclofen induces a persistent change in EPSC rectification. (**a**) Time course of effect of 3 μM baclofen on EPSC amplitude at –60 mV in a single cell. Filled symbols represent mean (averages of 1-min periods) and error bars represent s.e.m. Open symbols show response failures. Shaded area denotes the period of baclofen application. Note the short-lived depression of EPSC amplitude accompanied by an increase in failure rate and the small decrement in EPSC amplitude that persists after baclofen removal. (**b**) Representative averaged parallel fiber–evoked EPSCs (–60 mV, 10-ms interval) showing paired-pulse facilitation in control, during baclofen application and following baclofen wash. (**c**) Mean PPR increased in baclofen. Open symbols show individual cells, solid symbols show mean data; asterisk denotes significant difference from control ($P = 0.031$, see text). (**d**) Averaged parallel fiber–evoked EPSCs at –60 mV and +40 mV, before and following application of 3 μM baclofen (5 min). Control averages are from EPSCs recorded in a 5-min epoch immediately before application of baclofen (–60 mV) and in the preceding 5 min (+40 mV). Post-baclofen averages are from EPSCs recorded in a 5-min epoch starting 10 min after baclofen removal (–60 mV) and in the subsequent 5 min (+40 mV). Across cells, the post-baclofen epoch began between 8 and 18 min following baclofen removal. (**e**) Corresponding *I-V* plots: inwardly rectifying EPSCs (rectification index = 0.48) became less rectifying following baclofen (rectification index = 0.75). (**f**,**g**) Pooled data showing that the persistent action of baclofen involves elevation of intracellular $Ca^{2+}$. Baclofen reduced mean EPSC amplitude at –60 mV (–110.9 ± 13.1 pA in control versus –55.7 ± 5.6 pA in baclofen) and this effect, albeit significantly reduced, persisted following baclofen removal (–90.2 ± 13.5 pA, $n = 18$, $P = 0.0231$, Wilcoxon matched pairs). Baclofen increased rectification index during application (0.47 ± 0.05 in control versus 0.58 ± 0.05 in baclofen), and this effect persisted following baclofen removal (0.61 ± 0.07, $n = 15$, $P = 0.0023$, Wilcoxon matched pairs). The effect of baclofen on failure rate (0.21 ± 0.05 in control versus 0.63 ± 0.07 in baclofen) did not persist following baclofen removal (0.23 ± 0.07, $n = 14$, $P = 0.4887$, Wilcoxon matched pairs). (**g**) Summary data showing the effects of baclofen when recorded with intracellular BAPTA. Baclofen produced no persistent change in rectification index or amplitude (0.65 ± 0.04 and –83.8 ± 7.0 pA in control versus 0.63 ± 0.05 and –86.2 ± 6.3pA post-baclofen, $n = 8$). Baclofen still decreased amplitude and increased failure rate, but this was not sustained after washout. In **f** and **g**, error bars denote s.e.m. * indicates $P < 0.05$.

suggest that DHPG-induced changes in GluR2-containing AMPARs do not require $GABA_BR$ activation and that the effect of baclofen could reflect enhancement of ongoing (tonic) mGluR activity.

### Tonic metabotropic receptor activity sets CP-AMPAR basal tone

To determine whether group 1 mGluRs and $GABA_BRs$ are indeed tonically active, we examined the effects of mGluR1 and $GABA_BR$ blockers (**Fig. 5**). Tonic mGluR activity in stellate cells could reflect the presence of ambient glutamate (arising from spontaneous transmitter release, for example) or could indicate that mGluRs are constitutively active[35]. Competitive antagonists are expected to block mGluRs that are agonist activated, but not those that are constitutively active. The competitive mGluR1α antagonist LY367385 (**Fig. 5a**,**e**) produced a gradual (in less than 15 min) increase in mean EPSC amplitude (at –60 mV, from –91.1 ± 7.7 to –117.2 ± 13.5 pA, $n = 10$, $P = 0.0039$) and an increase in rectification (rectification index decreased from 0.51 ± 0.06 to 0.41 ± 0.05, $n = 9$, $P < 0.001$) (**Fig. 5b**,**e**).

Similarly, application of the competitive $GABA_BR$ blocker CGP62349 produced a significant enhancement of EPSC amplitude at −60 mV (from –116.7 ± 18.4 to –145.2 ± 22.4 pA in CGP62349, $n = 15$, $P = 0.0034$) and increase in EPSC rectification (rectification index decreased from 0.53 ± 0.05 to 0.41 ± 0.04, $n = 10$, $P = 0.0441$) (**Fig. 5c–e**). Consistent with the view that ambient GABA is present at sufficient levels to tonically activate $GABA_B$ receptors (both pre- and postsynaptic), the PPR was significantly decreased by 3 μM CGP (**Fig. 5f**,**g**). Thus, although the CGP62349-induced increase in EPSC amplitude can be ascribed in part to block of presynaptic $GABA_BRs$, the increase in EPSC rectification indicates a postsynaptic change in CP-AMPARs. These results are consistent with the idea that tonic metabotropic receptor activity, resulting from the action of ambient glutamate and GABA, regulates the basal level of CP-AMPARs that are present at parallel fiber–stellate cell synapses.

### Synaptic mGluR activation induces a loss of CP-AMPARs

Does synaptic activation of mGluRs trigger the subunit switch induced by high-frequency activity at parallel fiber–stellate cell synapses[3]? We monitored stellate cells throughout the period of high-frequency stimulation and observed a robust slow inward current that could be readily blocked with mGluR antagonists (100 μM 7-(Hydroxyimino) cyclopropa[b]chromen-1a-carboxylate ethyl ester (CPCCOEt) and 10 μM MPEP, or 100 μM LY367385 and 10 μM MPEP; **Fig. 6a**,**b**). In control conditions, most cells (8 out of 11) showed a clear slow current

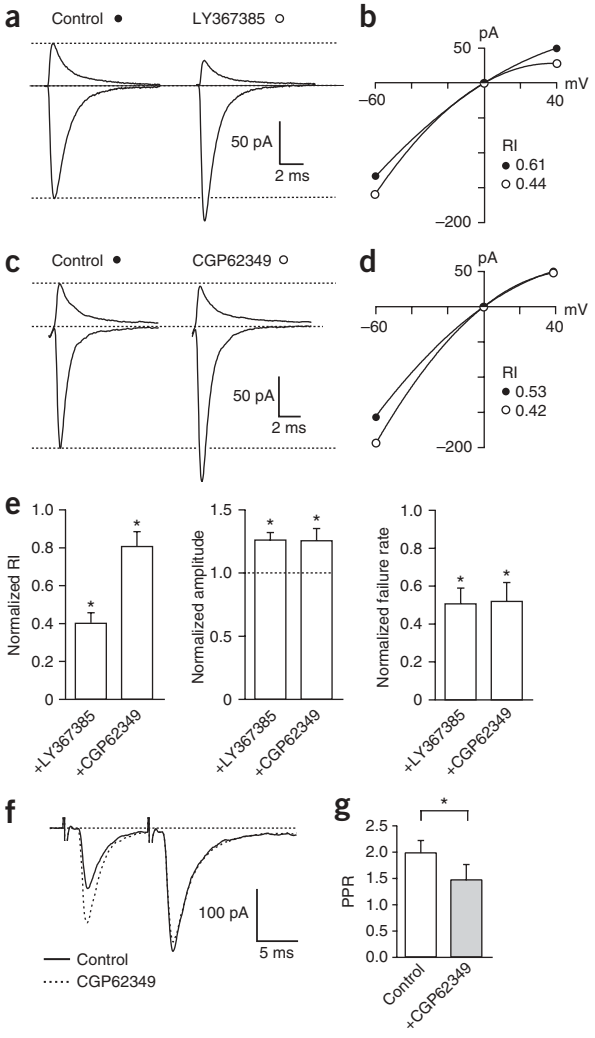


**Figure 5** mGluR and $GABA_B$ receptors are tonically active. (**a**) Averaged parallel fiber–evoked EPSCs at –60 mV and +40 mV, before and after application of LY367385 (100 μM). (**b**) Corresponding *I-V* plot. Inwardly rectifying EPSCs (control rectification index = 0.61) showed increased rectification in the presence of LY367385 (rectification index = 0.41). (**c**,**d**) As for **a** and **b**, but with CGP62349 (5 μM). Control inwardly rectifying EPSCs (rectification index = 0.53) showed increased rectification in the presence of CGP62349 (rectification index = 0.42). (**e**) Pooled data showing that LY367385 and CGP62349 both increased rectification (normalized rectification indexes = 0.41 ± 0.05 and 0.81 ± 0.07), increased EPSC amplitude at –60 mV (normalized amplitudes = 1.27 ± 0.05 and 1.26 ± 0.09) and reduced failure rate (normalized failure rate = 0.51 ± 0.08 and 0.52 ± 0.09) ($n$ = 10–15). (**f**) Parallel fiber–evoked EPSCs in control conditions and in the presence of 3 μM CGP62349 (–60 mV, 10-ms interval). (**g**) PPR was significantly decreased in the presence of 3 μM CGP62349 (from 2.00 ± 0.22 to 1.48 ± 0.28, $P$ = 0.0313, Wilcoxon matched pairs, $n$ = 6). In **e** and **g**, error bars denote s.e.m. * indicates $P < 0.05$.

(> 50 pA) in response to the train of stimuli, whereas no such current was seen in the presence of mGluR antagonists (in 11 cells).

To test whether synaptic mGluR activation can drive the AMPAR subunit change, we examined EPSCs before and after high-frequency stimulation in both control cells and in cells exposed to LY367385 and MPEP. As expected, high-frequency stimulation reduced EPSC amplitude (at –60 mV) in control conditions (from –91.7 ± 8.2 to –69.6 ± 5.5 pA, $n$ = 11, $P$ = 0.0015) and increased rectification index (from 0.37 ± 0.03 to 0.48 ± 0.04, $P$ = 0.0056) (**Fig. 6c–h**). In the presence of mGluR blockers, however, we found no significant change in either EPSC amplitude (–97.2 ± 15.0 pA versus –93.9 ± 14.3 pA, $P$ = 0.28, $n$ = 7) or rectification index (0.44 ± 0.05 versus 0.46 ± 0.07, $n$ = 7, $P$ = 0.68) (**Fig. 6e–h**). CGP62349 (10 μM) had no substantial

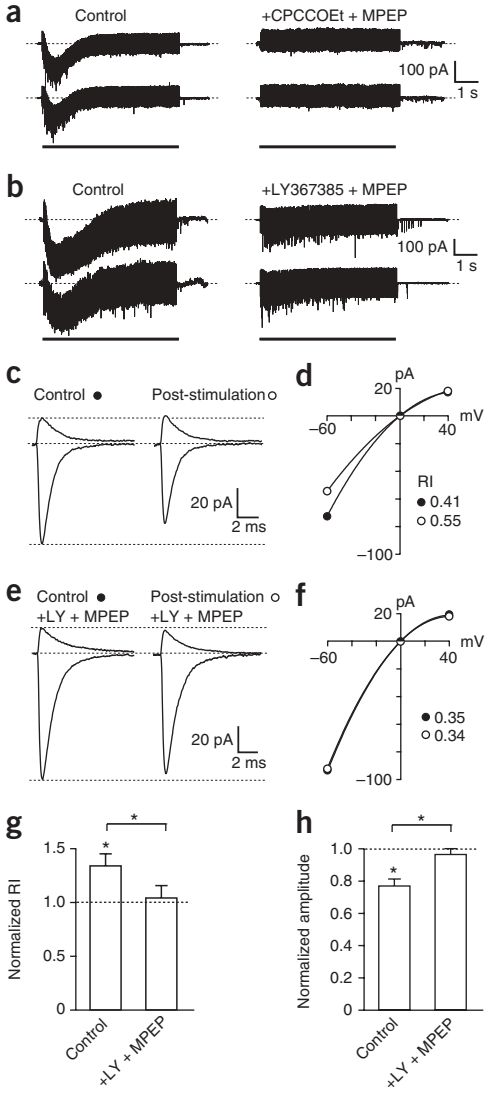


**Figure 6** Synaptic activation of mGluRs induces a change in AMPAR properties. (**a**) Slow inward currents evoked in a stellate cell (–60 mV) by high-frequency stimulation of parallel fibers (trains of 100 stimuli at 50 Hz, denoted by horizontal solid lines); rapid vertical deflections result from stimulus artifacts plus evoked EPSCs. Traces are from a representative cell, in which the slow currents were abolished by CPCCOEt (100 μM) and MPEP (10 μM). (**b**) Representative traces from a different cell, in which slow inward currents were abolished by LY3567385 (100 μM) and MPEP (10 μM). (**c**) Mean parallel fiber–evoked EPSCs at +40 and –60 mV from the same cell before and after high-frequency stimulation of the type shown in **a** and **b** (three trains of 100 stimuli at 50 Hz, separated by 10-s intervals). (**d**) *I-V* relationships for the data shown in **c**. (**e**,**f**) Same as **c** and **d**, but in the presence of LY367385 (100 μM) and MPEP (10 μM). (**g**,**h**) Pooled data showing that with mGluRs blocked, parallel fiber stimulation did not alter the rectification index or EPSC amplitude at –60 mV. The normalized rectification index and EPSC amplitude at –60 mV (1.35 ± 0.11 and 0.77 ± 0.04) were significantly altered in the presence of mGluR antagonists (1.05 ± 0.12 and 0.97 ± 0.03). In **g** and **h**, error bars denote s.e.m. * indicates $P < 0.05$).

effect on the synaptically induced mGluR inward current or on the resultant change in EPSC properties (data not shown), consistent with the view that $GABA_BR$ activation enhances, rather than enables, mGluR responses. Notably, mGluR activation alone was insufficient for the targeting of GluR2-containing AMPARs; $Ca^{2+}$ entry through AMPAR channels was essential for this process, as EPSCs are unchanged by high-frequency parallel fiber stimulation activity when $Ca^{2+}$-influx is inhibited[3].

## DISCUSSION

Regulation of CP-AMPARs may be important in a variety of forms of synaptic plasticity[3–7] and in neurological disorders[26,36]. Our results identify three key elements that underlie an activity-dependent switch in AMPAR subtype in cerebellar stellate cells. First, activation of both mGluRs and CP-AMPARs is necessary and sufficient to trigger this plasticity. Second, $GABA_BR$ activation can promote the loss of CP-AMPARs. Third, mGluRs and $GABA_BRs$ are both normally tonically activated by ambient transmitter, thereby limiting CP-AMPAR expression. Tonic activity of mGluRs and $GABA_BRs$ thus determines the ability of synapses to undergo this form of plasticity.

### Activation of both mGluRs and CP-AMPARs is necessary

Although the depolarization of stellate cells produced by short bursts of high-frequency parallel fiber activity[18] will limit $Ca^{2+}$ entry through CP-AMPARs[14], mGluR activation produces an additional rise in intracellular $Ca^{2+}$ that is voltage independent. The convergence of these two signals appears to be necessary to drive the changes in AMPAR subtype.

At parallel fiber–Purkinje cell synapses, activation of postsynaptic mGluRs is strongly regulated by glutamate uptake[37]. This appears to not be the case in stellate cells; here, although minimal stimulation of parallel fibers causes a small amount of glutamate to diffuse to extrasynaptic sites, a stimulus train results in substantial spill over[17,18]. Electron microscopy studies have shown mGluRs are generally distributed at the periphery of the postsynaptic density[38], an arrangement that is consistent with enhanced stellate cell mGluR activation during high-frequency parallel fiber activity. Furthermore, the structural features of the *en passant* parallel fiber–stellate cell synapse would appear to favor activation of mGluRs. At these synapses, the distance to glial transporters is long and the density of GLT1 and GLAST transporters is low[39], implying unhindered diffusion to extrasynaptic sites. This would allow mGluRs to be activated following brief bursts of high-frequency parallel fiber activity (which are known to occur, for example, in response to sensory stimulation[40,41]) and by the volume transmission recently found to be associated with climbing fiber activation[42].

### Comparison with other mGluR-dependent forms of plasticity

The mGluR/CP-AMPAR–induced plasticity that we describe differs fundamentally from the mGluR-induced long-term depression (LTD) that has been described in hippocampal CA1 cells and LTD at parallel fiber–Purkinje cell synapses. Although the mechanism of DHPG-induced LTD in the hippocampus remains uncertain and appears to be age dependent[43], it is thought to involve either reduced transmitter release[44] or loss of postsynaptic AMPARs[45,46] or both. Notably, it does not appear to involve any change in postsynaptic GluR2 targeting or AMPAR $Ca^{2+}$ permeability[44–46]. Similarly, parallel fiber–Purkinje cell LTD is thought to be expressed solely as a reduction in the number of functional AMPA receptors rather than as a change in GluR2 expression[47]. Presynaptic mGluR-induced LTD at parallel fiber–stellate cell synapses does not involve a switch in AMPAR subtype and requires signaling through CB1 receptors[33]. The postsynaptic AMPAR subunit switch that we found does not depend on synthesis of cannabinoids or activation of CB1Rs. The absence of the long-term presynaptic depression in our experiments is consistent with the view that cannabinoid release from stellate cells requires activation not only of mGluRs, but also of NMDARs[31]; the latter were blocked during our experiments. It seems likely that these two forms of plasticity coexist at parallel fiber–stellate cell synapses.

The form of plasticity described here shares certain features with the reversal of cocaine-induced strengthening of excitatory synapses onto dopamine cells in the ventral tegmental area (VTA). Recent work has shown that exposure to cocaine induces the expression of CP-AMPARs at VTA synapses. This change is rapidly reversed by mGluR activation[6], reflecting replacement of GluR2-lacking AMPARs with lower-conductance GluR2-containing AMPARs[27], as seen in stellate cells[3]. This raises the possibility that a common mechanism could underlie a switch in AMPAR subunit composition and $Ca^{2+}$ permeability under normal and pathological conditions. It is of note, however, that reversal of cocaine-induced synaptic plasticity requires de novo synthesis of GluR2 (ref. 27). In stellate cells, although we found that protein synthesis was required, extrasynaptic AMPARs are GluR2-containing and are therefore available to be incorporated at the synapse following lateral movement[3,5]. In this respect, it is of interest that a localized rise in $[Ca^{2+}]_i$ could regulate the synaptic accumulation of GluR2-containing AMPAR as a result of slow-down of intramembrane GluR2 movement[48]. Finally, dopamine cells in the VTA differ from stellate cells both in terms of their AMPAR subtypes and the fact that they express postsynaptic NMDARs[6].

It could be argued that, rather than reflecting a loss of CP-AMPARs, plasticity involving a change in rectification index might arise from a modification in the interaction of CP-AMPAR subunits with TARPs. We have recently shown that rectification of CP-AMPARs can be reduced by the interaction of homomeric GluR3 receptors (the main CP-AMPAR subtype that is thought to be present in these cells) with stargazin or other TARPS. For example, rectification of AMPARs could be rapidly modified if DHPG treatment triggered 'TARP-less' AMPARs to associate with TARPs and render them less sensitive to block by polyamines. Such a mechanism would require the initial presence of TARP-less CP-AMPARs. This seems unlikely, however, as our previous studies[14] have suggested that both CP-and CI-AMPARs have properties that are indicative of an association with TARPs at the parallel fiber–stellate cell synapse.

### Tonic mGluR and $GABA_BR$ activation regulates CP-AMPARs

Our findings establish that $GABA_BRs$ participate in the regulation of synaptic plasticity in stellate cells by enhancing mGluR activity, indicating that both excitatory and inhibitory inputs drive the dynamic change in AMPAR $Ca^{2+}$ permeability. Synergistic interaction between mGluRs and $GABA_BRs$ has been suggested as a possible mechanism for regulating synaptic plasticity at parallel fiber-Purkinje cell synapses[23]. The basis of this interaction remains unclear[23,49].

Coincident activation of mGluRs and $GABA_BRs$ could be particularly important in neuronal circuits where synaptic input provides both direct excitation and indirect feedforward inhibition, such as occurs in many interneurons, which express CP-AMPARs[9,15,50]. Furthermore, by controlling the relative proportion of CP-AMPARs, tonic activation of mGluRs and $GABA_BRs$ provides an unexpected mechanism for limiting the capacity of excitatory synapses to undergo plasticity involving postsynaptic CP-AMPARs.

## METHODS

**Slice preparation.** Coronal slices (200 μm) were made from the cerebellar vermis of postnatal day 18–21 Sprague-Dawley rats as described previously[14,17].

Following decapitation, in accordance with the UK Animals (Scientific Procedures) Act 1986, slices were cut in ice-cold slicing solution with a moving blade microtome (DTK-1000, Dosaka EM Company; HM 650V, Microm International GmbH). The solution contained 85 mM NaCl, 2.5 mM KCl, 0.5 mM $CaCl_2$, 4 mM $MgCl_2$, 25 mM $NaHCO_3$, 1.25 mM $NaH_2PO_4$, 64 mM sucrose, 25 mM glucose and 0.02 mM D-2-amino-5-phosphonopentanoic acid (D-AP5, Tocris Bioscience). This was bubbled with 95% $O_2$ and 5% $CO_2$, pH 7.4. The slices were then kept at 32 °C for 40 min. During the final 20 min of this period, the slicing solution was gradually exchanged with extracellular solution containing 125 mM NaCl, 2.5 mM KCl, 1.25 mM $NaH_2PO_4$, 26 mM $NaHCO_3$, 25 mM glucose, 2 mM $CaCl_2$ and 1 mM $MgCl_2$ (pH 7.4 when bubbled with 95% $O_2$ and 5% $CO_2$). Slices were then perfused with this solution at 22–25 °C for a further 20 min before recording. Whole-cell recordings were made from visually identified interneurons (presumptive stellate cells, located in the outer third of the molecular layer). Electrodes (5–10 MΩ resistance) contained 140 mM CsCl, 10 mM HEPES, 5 mM EGTA(Cs), 10 mM TEACl, 2 mM $Mg_2ATP$, 0.5 mM $CaCl_2$, 4 mM NaCl and 0.1 mM spermine, adjusted to pH 7.4 with CsOH, giving a final osmolarity of ~285 mOsm. Series resistance was monitored throughout each experiment, and if it changed by >20%, the data were discarded. EPSCs were evoked by parallel fiber stimulation using a patch electrode (3–5 MΩ) filled with external solution placed in the molecular layer; pulses of 20–200-μs duration (60–99 V) were applied at 0.5 Hz. Recordings were made at –60 mV at 22–25 °C in the presence of 20 μM D-AP5 and 20 μM bicuculline methobromide to isolate AMPAR-mediated currents. Signals were acquired with an Axopatch 200B amplifier, filtered to 2 kHz and digitized at 10 or 20 kHz (pClamp8 software, Molecular Devices). Once a stable baseline response was established, responses were obtained at a variety of membrane voltages, with 10-s epochs at different voltages being repeated in a pseudo-random fashion, before and after drug application (**Supplementary Fig. 1**). In most cases, such *I-V* determinations were restricted to –60 and +40 mV alone and separated by continuous measurement at –60 mV.

**Data analysis.** Data were analyzed using IGOR Pro (Wavemetrics) and NeuroMatic (http://www.neuromatic.thinkrandom.com/). Events were detected using threshold crossing in a window following the stimulus and were considered to be responses if the peak current was 3–5× the s.d. of the background noise. In practice, identification of failures was unambiguous. Average EPSCs were generated by aligning monotonically rising events on their 20% rise time. For plots of EPSC amplitude against time, selected events in 1-min epochs were averaged.

**Quantification of rectification.** The mean amplitudes of parallel fiber–evoked EPSCs (calculated excluding failures) were plotted against membrane potential and the *I-V* relationship fitted with a third-order polynomial constrained to cross the abscissa at the independently determined mean reversal potential (–1.5 ± 0.3 mV, $n = 32$). The rectification index was calculated by dividing the peak amplitude of the averaged EPSC obtained at the most positive voltage (typically +40 mV) by the extrapolated amplitude of the EPSC at a membrane voltage equidistant from the reversal potential (that is, rectification index = EPSC + 40/EPSC – 41.5). Thus, for a linear *I-V*, the rectification index equals 1, and, for an inwardly rectifying response, the rectification index is less than 1. The veracity of this approach was confirmed by comparing the rectification index values obtained by this method with those obtained from fitting EPSC amplitudes obtained at multiple voltages (–60, –40, –20, 0, +20 and +40 mV; **Supplementary Fig. 1**).

**Stability of EPSC amplitude and rectification index.** In experiments to examine whether elevated $[Ca^{2+}]_i$ was required for the mGluR-mediated loss of GluR2-lacking AMPARs, we first established that EPSCs evoked at low frequency (0.5Hz) with basal $Ca^{2+}$-buffering using EGTA showed no significant change in amplitude or rectification index over prolonged recordings. In a control period, the mean EPSC amplitude at –60 mV (measured over a 5 min epoch) was –154.8 ± 21.4 pA. After a further 10 min of recording, the mean amplitude (measured over a 5-min epoch, from 15 to 20 min) was –139.2 ± 22.8pA ($n = 6$, $P = 0.8125$, Wilcoxon matched pairs). The corresponding rectification index values were 0.53 ± 0.08 and 0.48 ± 0.08 ($P = 0.875$).

**mGluR antagonists.** In experiments to test whether mGluR activation participates in insertion of GluR2-containing AMPARs, we measured EPSC properties following application of DHPG (50 μM) and examined the action of LY367385 (100 μM). Although mGluR5 receptors have not been described in stellate cells[22], in some experiments, we also included MPEP (10 μM) to exclude the possibility of activating any group 1 mGluRs. In these conditions, following DHPG treatment, the mean normalized change in EPSC amplitude at –60 mV (1.02 ± 0.08) and rectification index (1.15 ± 0.13) indicated an effective block of the DHPG effect ($n = 4$, both $P = 0.813$, Wilcoxon matched pairs).

**Failure rate.** This was calculated by dividing the number of failures by the number of stimuli for a given time period. Paired-pulse ratio (PPR) was determined by dividing the amplitude of the second EPSC (A2) by the amplitude of the first (A1; PPR = mean of A2/mean of A1). In this case, amplitudes were taken from averages constructed using all sweeps in a given condition without alignment. mEPSCs, recorded in the presence of 0.3 μM tetrodotoxin, were detected using a scaled template algorithm (NeuroMatic) and aligned as for evoked EPSCs.

Data are expressed as mean ± s.e.m. When data were distributed normally (Shapiro-Wilk test), statistical differences between groups were determined using a two-tailed paired or unpaired Student's *t*-test, as appropriate. Alternatively, nonparametric tests were used as indicated. Differences were considered to be significant at $P < 0.05$.

*Note: Supplementary information is available on the Nature Neuroscience website.*

**ACKNOWLEDGMENTS**

We thank C. Bats, P. Chadderton, B. Clark and D. Soto for helpful discussion and comments on the manuscript. This work was supported by a Wellcome Trust Programme Grant (S.G.C.-C. and M.F.), a Wellcome Trust Studentship (L.K.) and a Royal Society-Wolfson Research Award (S.G.C.-C.).

Published online at http://www.nature.com/natureneuroscience/
Reprints and permissions information is available online at http://www.nature.com/reprintsandpermissions/

1. Bredt, D.S. & Nicoll, R.A. AMPA receptor trafficking at excitatory synapses. *Neuron* **40**, 361–379 (2003).
2. Collingridge, G.L., Isaac, J.T. & Wang, Y.T. Receptor trafficking and synaptic plasticity. *Nat. Rev. Neurosci.* **5**, 952–962 (2004).
3. Liu, S.Q. & Cull-Candy, S.G. Synaptic activity at calcium-permeable AMPA receptors induces a switch in receptor subtype. *Nature* **405**, 454–458 (2000).
4. Lei, S. & McBain, C.J. Two Loci of expression for long-term depression at hippocampal mossy fiber-interneuron synapses. *J. Neurosci.* **24**, 2112–2121 (2004).
5. Gardner, S.M. *et al.* Calcium-permeable AMPA receptor plasticity is mediated by subunit-specific interactions with PICK1 and NSF. *Neuron* **45**, 903–915 (2005).
6. Bellone, C. & Luscher, C. Cocaine triggered AMPA receptor redistribution is reversed *in vivo* by mGluR-dependent long-term depression. *Nat. Neurosci.* **9**, 636–641 (2006).
7. Ge, W.P. *et al.* Long-term potentiation of neuron-glia synapses mediated by $Ca^{2+}$-permeable AMPA receptors. *Science* **312**, 1533–1537 (2006).
8. Ho, M.T. *et al.* Developmental expression of Ca2+-permeable AMPA receptors underlies depolarization-induced long-term depression at mossy fiber CA3 pyramid synapses. *J. Neurosci.* **27**, 11651–11662 (2007).
9. Geiger, J.R. *et al.* Relative abundance of subunit mRNAs determines gating and $Ca^{2+}$ permeability of AMPA receptors in principal neurons and interneurons in rat CNS. *Neuron* **15**, 193–204 (1995).
10. Swanson, G.T., Kamboj, S.K. & Cull-Candy, S.G. Single-channel properties of recombinant AMPA receptors depend on RNA editing, splice variation and subunit composition. *J. Neurosci.* **17**, 58–69 (1997).
11. Bowie, D., Lange, G.D. & Mayer, M.L. Activity-dependent modulation of glutamate receptors by polyamines. *J. Neurosci.* **18**, 8175–8185 (1998).
12. Rozov, A. & Burnashev, N. Polyamine-dependent facilitation of postsynaptic AMPA receptors counteracts paired-pulse depression. *Nature* **401**, 594–598 (1999).
13. Aizenman, C.D., Muñoz-Elías, G. & Cline, H.T. Visually driven modulation of glutamatergic synaptic transmission is mediated by the regulation of intracellular polyamines. *Neuron* **34**, 623–634 (2002).
14. Soto, D., Coombs, I.D., Kelly, L., Farrant, M. & Cull-Candy, S.G. Stargazin attenuates intracellular polyamine block of calcium-permeable AMPA receptors. *Nat. Neurosci.* **10**, 1260–1267 (2007).
15. Jonas, P., Bischofberger, J., Fricker, D. & Miles, R. Interneuron Diversity series: Fast in, fast out—temporal and spatial signal processing in hippocampal interneurons. *Trends Neurosci.* **27**, 30–40 (2004).
16. Chávez, A.E., Singer, J.H. & Diamond, J.S. Fast neurotransmitter release triggered by Ca influx through AMPA-type glutamate receptors. *Nature* **443**, 705–708 (2006).

17. Clark, B.A. & Cull-Candy, S.G. Activity-dependent recruitment of extrasynaptic NMDA receptor activation at an AMPA receptor-only synapse. *J. Neurosci.* **22**, 4428–4436 (2002).
18. Carter, A.G. & Regehr, W.G. Prolonged synaptic currents and glutamate spillover at the parallel fiber to stellate cell synapse. *J. Neurosci.* **20**, 4423–4434 (2000).
19. Mittmann, W., Koch, U. & Hausser, M. Feed-forward inhibition shapes the spike output of cerebellar Purkinje cells. *J. Physiol. (Lond.)* **563**, 369–378 (2005).
20. Mann-Metzer, P. & Yarom, Y. Pre- and postsynaptic inhibition mediated by GABA(B) receptors in cerebellar inhibitory interneurons. *J. Neurophysiol.* **87**, 183–190 (2002).
21. Rancillac, A. & Crepel, F. Synapses between parallel fibres and stellate cells express long-term changes in synaptic efficacy in rat cerebellum. *J. Physiol. (Lond.)* **554**, 707–720 (2004).
22. Karakossian, M.H. & Otis, T.S. Excitation of cerebellar interneurons by group I metabotropic glutamate receptors. *J. Neurophysiol.* **92**, 1558–1565 (2004).
23. Hirono, M., Yoshioka, T. & Konishi, S. GABA(B) receptor activation enhances mGluR-mediated responses at cerebellar excitatory synapses. *Nat. Neurosci.* **4**, 1207–1216 (2001).
24. Häusser, M. & Clark, B.A. Tonic synaptic inhibition modulates neuronal output pattern and spatiotemporal synaptic integration. *Neuron* **19**, 665–678 (1997).
25. Nusser, Z., Cull-Candy, S. & Farrant, M. Differences in synaptic $GABA_A$ receptor number underlie variation in GABA mini amplitude. *Neuron* **19**, 697–709 (1997).
26. Feldmeyer, D. *et al.* Neurological dysfunctions in mice expressing different levels of the Q/R site-unedited AMPAR subunit GluR-B. *Nat. Neurosci.* **2**, 57–64 (1999).
27. Mameli, M., Balland, B., Lujan, R. & Luscher, C. Rapid synthesis and synaptic insertion of GluR2 for mGluR-LTD in the ventral tegmental area. *Science* **317**, 530–533 (2007).
28. Noel, J. *et al.* Surface expression of AMPA receptors in hippocampal neurons is regulated by an NSF-dependent mechanism. *Neuron* **23**, 365–376 (1999).
29. Bähring, R. & Mayer, M.L. An analysis of philanthotoxin block for recombinant rat GluR6(Q) glutamate receptor channels. *J. Physiol. (Lond.)* **509**, 635–650 (1998).
30. Chevaleyre, V., Takahashi, K.A. & Castillo, P.E. Endocannabinoid-mediated synaptic plasticity in the CNS. *Annu. Rev. Neurosci.* **29**, 37–76 (2006).
31. Beierlein, M. & Regehr, W.G. Local interneurons regulate synaptic strength by retrograde release of endocannabinoids. *J. Neurosci.* **26**, 9935–9943 (2006).
32. Hashimotodani, Y., Ohno-Shosaku, T., Maejima, T., Fukami, K. & Kano, M. Pharmacological evidence for the involvement of diacylglycerol lipase in depolarization-induced endocanabinoid release. *Neuropharmacology* **54**, 58–67 (2008).
33. Soler-Llavina, G.J. & Sabatini, B.L. Synapse-specific plasticity and compartmentalized signaling in cerebellar stellate cells. *Nat. Neurosci.* **9**, 798–806 (2006).
34. Liu, S.J. & Cull-Candy, S.G. Subunit interaction with PICK and GRIP controls $Ca^{2+}$ permeability of AMPARs at cerebellar synapses. *Nat. Neurosci.* **8**, 768–775 (2005).
35. Ango, F. *et al.* Agonist-independent activation of metabotropic glutamate receptors by the intracellular protein Homer. *Nature* **411**, 962–965 (2001).
36. Hartmann, B. *et al.* The AMPA receptor subunits GluR-A and GluR-B reciprocally modulate spinal synaptic plasticity and inflammatory pain. *Neuron* **44**, 637–650 (2004).
37. Brasnjo, G. & Otis, T.S. Neuronal glutamate transporters control activation of post-synaptic metabotropic glutamate receptors and influence cerebellar long-term depression. *Neuron* **31**, 607–616 (2001).
38. Baude, A. *et al.* The metabotropic glutamate receptor (mGluR1α) is concentrated at perisynaptic membrane of neuronal subpopulations as detected by immunogold reaction. *Neuron* **11**, 771–787 (1993).
39. Chaudhry, F.A. *et al.* Glutamate transporters in glial plasma membranes: highly differentiated localizations revealed by quantitative ultrastructural immunocytochemistry. *Neuron* **15**, 711–720 (1995).
40. Chadderton, P., Margrie, T.W. & Hausser, M. Integration of quanta in cerebellar granule cells during sensory processing. *Nature* **428**, 856–860 (2004).
41. Jörntell, H. & Ekerot, C.F. Properties of somatosensory synaptic integration in cerebellar granule cells *in vivo*. *J. Neurosci.* **26**, 11786–11797 (2006).
42. Szapiro, G. & Barbour, B. Multiple climbing fibers signal to molecular layer interneurons exclusively via glutamate spillover. *Nat. Neurosci.* **10**, 735–742 (2007).
43. Nosyreva, E.D. & Huber, K.M. Developmental switch in synaptic mechanisms of hippocampal metabotropic glutamate receptor–dependent long-term depression. *J. Neurosci.* **25**, 2992–3001 (2005).
44. Zakharenko, S.S., Zablow, L. & Siegelbaum, S.A. Altered presynaptic vesicle release and cycling during mGluR-dependent LTD. *Neuron* **35**, 1099–1110 (2002).
45. Xiao, M.Y., Zhou, Q. & Nicoll, R.A. Metabotropic glutamate receptor activation causes a rapid redistribution of AMPA receptors. *Neuropharmacology* **41**, 664–671 (2001).
46. Moult, P.R. *et al.* Tyrosine phosphatases regulate AMPA receptor trafficking during metabotropic glutamate receptor–mediated long-term depression. *J. Neurosci.* **26**, 2544–2554 (2006).
47. Linden, D.J. The expression of cerebellar LTD in culture is not associated with changes in AMPA-receptor kinetics, agonist affinity or unitary conductance. *Proc. Natl. Acad. Sci. USA* **98**, 14066–14071 (2001).
48. Borgdorff, A.J. & Choquet, D. Regulation of AMPA receptor lateral movements. *Nature* **417**, 649–653 (2002).
49. Kamikubo, Y. *et al.* Postsynaptic GABAB receptor signaling enhances LTD in mouse cerebellar Purkinje cells. *J. Physiol. (Lond.)* **585**, 549–563 (2007).
50. Lawrence, J.J. & McBain, C.J. Interneuron diversity series: containing the detonation–feedforward inhibition in the CA3 hippocampus. *Trends Neurosci.* **26**, 631–640 (2003).